Epilepsia, **47**(7):1144–1152, 2006
Blackwell Publishing, Inc.

Neocortical Hyperexcitability in a Genetic Model of Absence Seizures and Its Reduction by Levetiracetam

*Giovanna D'Arcangelo, *Margherita D'Antuono, *Virginia Tancredi, and †‡Massimo Avoli

*Dipartimento di Neuroscienze, Università di Roma "Tor Vergata," †Dipartimento di Fisiologia Umana e Farmacologia, Università di Roma "La Sapienza," Rome, Italy; and ‡Montreal Neurological Institute and Departments of Neurology and Neurosurgery and Physiology, McGill University, Montréal, Québec, Canada

Summary: *Purpose:* To study the effect of the antiepileptic drug levetiracetam (LEV) on the patterns of intrinsic optical signals (IOSs) generated by slices of the somatosensory cortex obtained from 3- and 6-month-old WAG/Rij and age-matched, nonepileptic control (NEC) rats.

Methods: WAG/Rij and NEC animals were anesthetized with enfluorane and decapitated. Brains were quickly removed, and neocortical slices were cut coronally with a vibratome, transferred to a submerged tissue chamber, and superfused with oxygenated artificial cerebrospinal fluid (aCSF). Slices were illuminated with a dark-field condensor and examined with a $\times 2.5$ objective; images were processed with a real time digital video image-enhancement system. Images were acquired before (background) and during electrical stimulation with a temporal resolution of 10 images/s and were displayed in pseudocolors. Extracellular stimuli (200 μs; <4 V) were delivered through bipolar stainless steel electrodes placed in the white matter.

Results: IOSs recorded in NEC slices bathed in control aCSF became less intense and of reduced size with age ($p < 0.05$); this trend was not seen in WAG/Rij slices. Age-dependent decreases in IOS intensity and area size were also seen in NEC slices superfused with aCSF containing the convulsant 4-aminopyridine (4-AP, 5 μM); in contrast, significant increases in both parameters occurred with age in 4-AP–treated WAG/Rij slices ($p < 0.05$). Under any of these conditions, the IOS intensity and area size slices were larger in WAG/Rij than in NEC slices. LEV (50–500 μM) application to WAG/Rij slices caused dose-dependent IOS reductions that were evident both in control and in 4-AP–containing aCSF and were more pronounced in 6-month-old tissue.

Conclusions: These data demonstrate age-dependent IOS modifications in NEC and WAG/Rij rat slices and identify a clear pattern of hyperexcitability that occurs in 6-month-old WAG/Rij neocortical tissue, an age when absence seizures occur in all animals. The ability of LEV to reduce these patterns of network hyperexcitability supports the potential use of this new antiepileptic drug in primary generalized epileptic disorders. **Key Words:** Levetiracetam—Intrinsic optical signals—Absence epilepsy.

Absence epilepsy is a neurologic disorder characterized by brief periods of impaired consciousness that are accompanied by generalized 3-Hz spike-and-wave (SW) discharges (1). The cellular mechanisms underlying generalized SW discharges have been extensively analyzed in animals (most often cats) that were made acutely epileptic by convulsant application or by low-frequency electrical stimuli (see for review: 2,3). More recently, these studies have been extended to rodents that are genetically predisposed to generate absence seizures. These models include the Genetic Absence Epilepsy in Rats from Strasbourg (GAERS) (4) and the Wistar Albino Glaxo/Rijswijk (WAG/Rij) rats (5,6). GAERS and WAG/Rij animals respond to antiabsence drugs in a way similar to what is seen in patients with primary generalized epilepsy, where a genetic component has been established (7,8).

Evidence obtained from normal animals that were treated for the short term with either convulsants or anesthetic agents (9–13) and from genetically predisposed rodents (4,14–17) indicates that hyperexcitable neocortical networks play a major role in SW-discharge initiation and propagation. Indeed, Meeren et al. (18) identified a "consistent cortical focus" for SW activity within the perioral area in the WAG/Rij somatosensory cortex (see also 19). Similar conclusions have been reached by Manning et al. (20) in the GAERS model. Moreover, by using a thalamocortical slice preparation, we found that the ability of epileptic WAG/Rij rat slices to generate slow rhythmic oscillations in the presence of low concentrations of 4-aminopyridine (4-AP) depends on the functional integrity of neocortical networks (21). This slow in vitro synchronous oscillatory activity was not recorded in slices

Accepted February 23, 2006.
‡Address correspondence and reprint requests to Dr. M. Avoli at Montreal Neurological Institute, 3801 University Street, Montreal, Quebec H3A 2B4, Canada. E-mail: massimo.avoli@mcgill.ca
doi: 10.1111/j.1528-1167.2006.00588.x

obtained from age-matched, nonepileptic control (NEC) Wistar rats.

The goal of our study was further to characterize with intrinsic optical signal (IOS) recording the hyperexcitable characteristics of neocortical slices obtained from 3- and 6-month-old WAG/Rij rats by comparing them with those identified in age-matched NECs. The choice of these two ages was dictated by in vivo evidence showing that absence seizures (and the accompanying generalized SW discharges) occur rarely in young WAG/Rij rats, but are always present in animals >180 days old (22). By using IOS recordings, which detect the changes in light scattering properties and absorption secondary to cell swelling (23–27), we attempted to quantify the intensity and spatial characteristics of the stimulus-induced responses generated by the four types of neocortical slices both under control conditions and in the presence of 4-AP. In addition, we analyzed the effects induced by levetiracetam (LEV) on the IOS patterns generated by 3- and 6-month-old WAG/Rij slices superfused with either control or 4-AP–containing medium. LEV is a novel antiepileptic drug (AED) characterized by a preclinical profile that is distinct from all other AEDs (28) and by repeatedly proven clinical efficacy that may include generalized epileptic disorders (29–31).

METHODS

Twelve and 10 WAG/Rij rats (Harlan, Horst, The Netherlands) aged 90 to 100 and 180–190 days old, respectively, as well as age-matched NEC rats [eight and seven animals for each group, respectively; strain: Crl(WI)BR Wistar; obtained from Harlan, Horst, The Netherlands] were used according to the procedures established by the European Union Councils of Animal Care. All efforts were made to minimize the number of animals used and their suffering. We also analyzed the behavior of NEC and WAG/Rij rats housed before performing the in vitro experiment. By doing so, we could document that all 180- to 190-day-old WAG/Rij rats (termed thereafter 6-month-old animals) displayed frequent episodes (duration ≤15 s) of behavioral arrest accompanied by mild myoclonic twitches. Previous in vivo studies have demonstrated that these clinical events correspond to bilaterally generalized SW discharges at 7–11 Hz (32,33). By contrast, similar episodes were rarely observed in 90- to 100-day-old WAG/Rij rats (termed thereafter 3-month-old animals) or in NEC rats regardless of age. These latter animals were not used for the experiments reported here.

WAG/Rij and NEC animals were anesthetized with enfluorane and decapitated. Their brains were quickly removed and placed in cold, oxygenated artificial cerebral spinal fluid (aCSF). Neocortical slices (450 μm) were cut coronally with a vibratome from a region corresponding to the somatosensory cortex that matched the plates reported by Paxinos and Watson (34) at –0.3 to +0.7 mm from the bregma (cf. also, 15,20). Slices were then transferred to a submerged tissue chamber and superfused with oxygenated aCSF (95% O_2/5% CO_2) at 32–34°C (pH 7.4). aCSF composition was in m*M*: NaCl 124, KCl 2, KH_2PO_4 1.25, $MgSO_4$ 1, $CaCl_2$ 2, $NaHCO_3$ 26, and glucose 10. aCSF could also contain 4-AP (5 μM) and/or LEV (50–500 μM).

The slices were illuminated with a dark-field condensor and examined with a ×2.5 objective; the illumination light was filtered with a bandpass interference filter (750 ± 50 nm). To detect IOS changes, analog contrast enhancement, background subtraction, and a fivefold digital enhancement were applied on line to video images that were obtained from an infrared video camera (C2400-07; Hamamatsu Photonics, Hamamatsu City, Japan). Images were processed with a real-time digital video image-enhancement system (Argus 20; Hamamatsu Photonics). Averaged dark-field images obtained under basal condition were digitized at 16 bits, stored on a personal computer, and then subtracted in real time from the incoming image before and at successive times after single-shock or tetanic electrical stimulation. Images were acquired before (background) and during electrical stimulation with a temporal resolution of 10 images/s and were displayed in pseudocolors, assigning a color look-up table to the relative pixel values (cf. 35). Data were further analyzed off-line with the software IAS2000 (Delta Sistemi, Roma, Italy) to quantify both the intensity and the area of the IOS changes in windows that covered the region of the slice where the change in IOS was detectable. IOS intensity was measured by calculating the difference between pixel intensity in each region of interest, and it was expressed as percentage of the digital intensity of the control (background) image of that series, by using the following formula: [(Tt – T0)/T0] ×100 (where T0 corresponds to the initial image of the series considered as background, and Tt is the image acquired at given time t after the end of the stimulus).

Extracellular stimuli (200 μs; <4 V) were delivered through bipolar stainless steel electrodes placed in the underlying white matter either as a single shock or as brief trains (50 Hz for 2 s). Selected portions of the neocortical layers in WAG/Rij slices were cut under visual control with a razor blade mounted on a micromanipulator. Measurements throughout the text are expressed as mean ± SD, and n represents the number of slices studied. Data were compared with the Student's *t* test or the analysis of variance (ANOVA) test and were considered significantly different if $p < 0.05$.

RESULTS

Stimulus-induced IOS generated by neocortical slices superfused with normal aCSF

As previously reported for experiments performed in 30- to 40-day-old rats (26,36), brief trains of stimuli delivered into the white matter during application of normal

aCSF, induced in 3-month-old NEC neocortical slices (n = 8) IOS changes that (a) reached maximal intensity within 2–4 s (3 ± 0.7 s; mean ± SD; n = 8) after the end of the stimulation; (b) decreased to baseline levels in 42–60 s; and (c) were characterized by a columnar-like representation with a peak increase localized in the superficial layers (Fig. 1Aa). Under analogous experimental conditions, neocortical slices (n = 7) obtained from 6-month-old animals responded to stimulus trains with IOS increases that had a comparable time course (i.e., peak latency, 2.9 ± 0.8 s; recovery within 45–70 s), but were not clearly delimited (Fig. 1Ab). Moreover, these IOSs displayed intensity values and areas sizes that were significantly lower and smaller, respectively, than in the experiments performed in 3-month-old rat slices. The characteristics of the IOSs recorded in 3- and 6-month-old NEC slices (n = 8 and 7, respectively) are quantified in terms of maximal IOS intensity and IOS area in panels C and D of Fig. 1. It must be emphasized that single-shock stimuli did not induce any consistent IOS changes in NEC slices obtained from both age-groups (not shown).

In contrast, IOS changes were consistently induced by single-shock stimuli in WAG/Rij neocortical slices obtained from 3- or 6-month-old animals, thus suggesting that these neocortical networks were hyperexcitable as compared with age-matched NECs (Fig. 1B). These IOS patterns had time courses similar to those seen in NEC slices after brief trains of stimuli. However, at variance to the IOS patterns observed in 3-month-old NEC tissue, IOS changes in age-matched WAG/Rij slices did not have any columnar delimitation (which was also true when stimulus trains were used; not shown). As illustrated in Fig. 1B, WAG/Rij slices obtained from 3- (n = 12) and 6-month-old (n = 11) animals generated similar patterns of IOS changes (cf. also Fig. 1E and F, where the peak increases and area sizes were quantified in the two

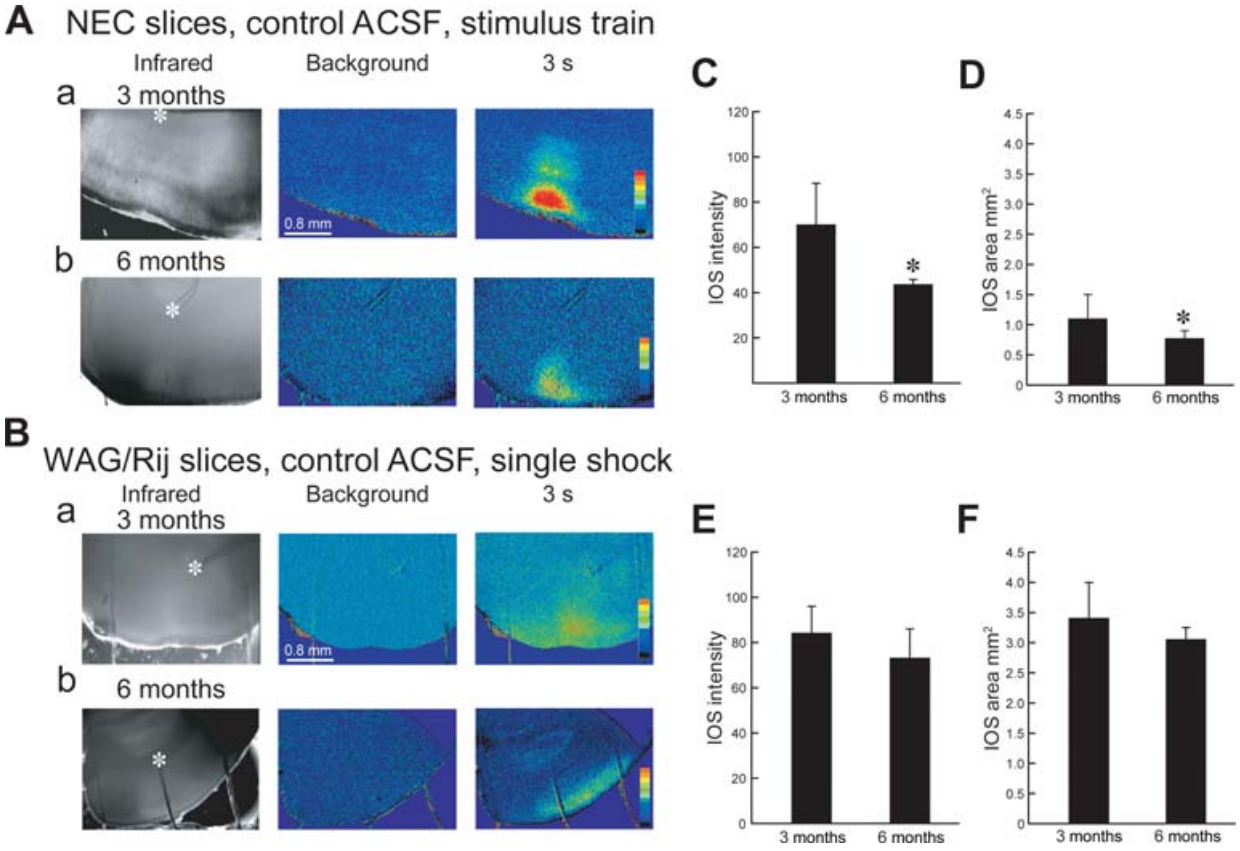

FIG. 1. Stimulus-induced intrinsic optical signals (IOSs) recorded in control artificial cerebrospinal fluid from neocortical slices obtained from NEC **(A)** and WAG/Rij **(B)** rats of different age groups. Under these conditions, stimulus trains were required to induce IOS changes in NEC slices. Note that in the 3-month-old experiment **(Aa)**, the IOS pattern recorded 3 s after the stimulus is characterized by a columnar representation with a peak increase localized in the superficial layers, as well as that in the 6-month-old slice **(Ab)**, the IOS increases attain lower peak values, have smaller areas sizes, and are not clearly delimited. Note also that single-shock stimuli in the WAG/Rij experiments cause widespread IOS activation with no columnar delimitation in both 3-month **(Ba)** and 6-month-old slices **(Bb)**. In this and the following figures, the position of the stimulating electrode is highlighted by an *asterisk*. **C, D:** Quantification of the intensity and area size of the IOS recorded in 3- and 6-month-old NEC slices (n = 8 and 7, respectively). Note that both parameters decrease significantly with age. **E, F:** Quantification of the intensity and area size of the IOS recorded in 3- and 6-month-old WAG/Rij slices (n = 12 and 11, respectively). Note that these parameters are not significantly different in the two age groups. In this and the following figures, $p < 0.05$ and $p < 0.02$ are indicated by single and double asterisks, respectively.

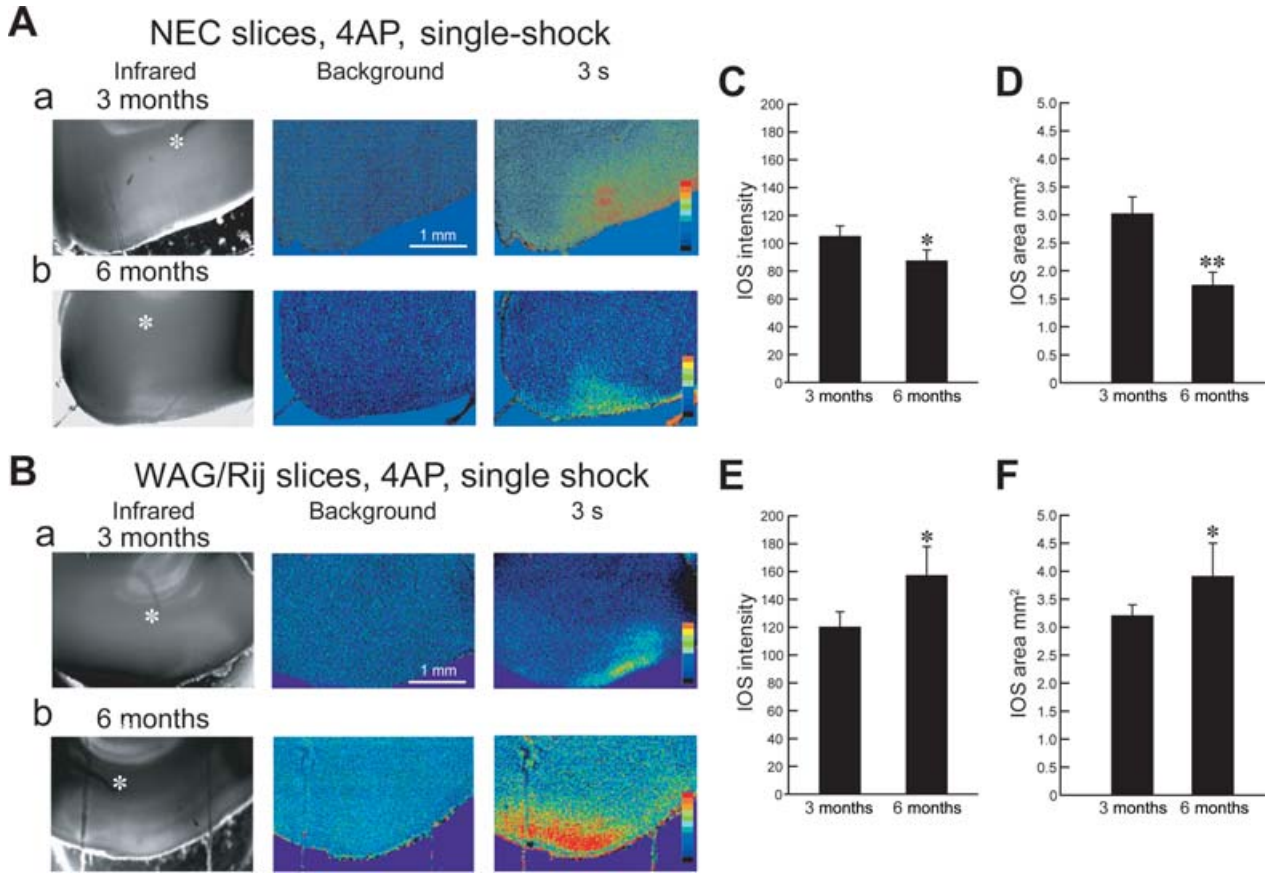

FIG. 2. Stimulus-induced intrinsic optical signals (IOSs) generated by NEC **(A)** and WAG/Rij **(B)** neocortical slices during application of 4-AP–containing artificial cerebrospinal fluid (aCSF). Stimuli in both strains were single-shock. Note that under these conditions, the IOS patterns recorded in 3- **(Aa)** and 6- **(Ab)** month-old NEC slices are widespread and more intense as compared with those obtained in normal aCSF in Fig. 1A. Note also in **Ba** and **Bb**, that the IOS changes recorded in the WAG/Rij experiments become more intense and wider with age. **C, D:** Quantification of the peak intensity and area size of the IOSs recorded in 3- and 6-month-old NEC slices in the presence of 4-AP ($n = 6$ and 6, respectively). Note that both parameters decrease with age, but only the IOS area values reach statistic significance. **E, F:** Quantification of the peak intensity and area size of the IOSs recorded in 3- and 6-month-old WAG/Rij slices ($n = 10$ and 13, respectively) superfused with 4-AP–containing medium. Note that at variance with what is seen in NEC experiments, both IOS peak intensity and area size values are significantly ($p < 0.02$) larger in slices obtained from 6-month-old WAG/Rij rats.

age groups). Hence, in contrast to that observed in NEC slices, WAG/Rij neocortical tissue did not show an age-dependent downregulation of the stimulus-induced IOSs. It should also be noted that the widespread IOS changes seen in WAG/Rij necortical slices were mainly localized to the superficial layers.

Stimulus-induced IOSs generated by neocortical slices during application of 4-AP–containing aCSF

We also analyzed the IOS changes induced by single-shock stimuli in NEC and WAG/Rij neocortical slices that were superfused with medium containing 4-AP. Under these experimental conditions, NEC slices obtained from 3- and 6-month-old rats ($n = 6$ and 6, respectively) generated IOS patterns that attained peak intensity within 3 s from the stimulus and decreased to baseline levels in ~70 s, but were more intense and widespread than was observed when these slices were tested with stimulus trains in the presence of normal medium (Fig. 2A). Thus during application of 4-AP, the IOS changes recorded in 3-month-old slices extended over the columnar organization identified at this age in normal medium and included areas up to 3 mm^2. However, by comparing the IOS changes induced by single-shock stimuli in the two age groups, we identified also in the presence of 4-AP an age-dependent decrease in peak intensity (marginally significant) and area size ($p < 0.01$). These characteristics are quantified in Fig. 2C and D.

Stimulus-induced, widespread IOSs were also seen in WAG/Rij neocortical slices superfused with 4-AP–containing medium ($n = 10$ and 13 obtained from 3- and 6-month-old WAG/Rij rats, respectively). However, in contrast to NEC slices, we found that both the IOS peak intensity and the area size were significantly larger in neocortical tissue that was obtained from 6-month-old WAG/Rij rats (Fig. 2B, E, and F). These findings indicate therefore that during aging, WAG/Rij rat neocortical

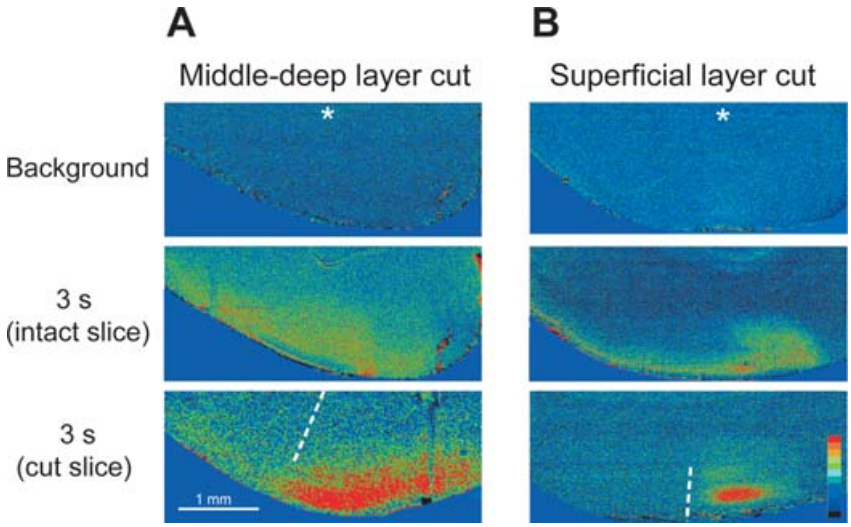

FIG. 3. Intrinsic optical signal (IOS) spread in 6-month-old WAG/Rij neocortical slices depend on intact supragranular layers. **A, B:** Two experiments carried out in 6-month-old WAG/Rij neocortical slices superfused with 4-AP. The IOS generated in the intact slices after single-shock stimuli are shown in the middle row, whereas in the bottom row, the IOS responses were recorded after cutting the middle/deep layers **(A)** or the supragranular layers **(B)**. The localization and extent of the cut is indicated by the dotted line. Note that the IOS signals remain ipsilateral to the stimulating electrode when the supragranular layers are cut.

networks do not display the decrease in network excitability seen to occur in NECs. In addition, by measuring the ratios of the IOS increases and of the area sizes identified in slices obtained from NEC and WAG/Rij rats of similar ages, we found that both parameters were consistently larger in WAG/Rij rat slices regardless of age, both in normal medium and in the presence of 4-AP (not shown).

Spread of the IOS responses obtained from 6-month-old WAG/Rij neocortical slices

A hallmark of the IOS responses induced in WAG/Rij rat slices both in control medium and in the presence of 4-AP is their horizontal spread. Hence we used delimited cuts of neocortical layers in 6-month-old WAG/Rij rat slices superfused with 4-AP–containing medium, to identify the layers through which such spread occurred. As shown in Fig. 3, the horizontal spread of the IOS changes induced by single-shock stimuli was not influenced by cutting the neocortical slice along a line normal to the pia that left intact the connections that are presumably running through the supragranular layers ($n = 4$). In contrast, the IOS signals remained ipsilateral to the stimulating electrode when the cut was performed at the level of the superficial layers ($n = 6$). Similar data were obtained by analyzing the spread of the stimulus-induced IOS changes generated by these WAG/Rij rat slices after prolonged (>80 min) 4-AP washout (not illustrated).

Effects of LEV on WAG/Rij rat neocortical slices superfused with 4-AP–containing aCSF

Finally, we studied the effects induced by the AED LEV on the IOS changes induced by single-shock stimuli in neocortical WAG/Rij slices that were superfused with either normal or 4-AP–containing aCSF. After recording stable IOS signals, we bath applied LEV at different doses for ≥20 min and repeated the stimulation procedure. As shown in Fig. 4A and B, 50 μM LEV reduced the intensity and the area of the IOS changes generated by both 3-month ($n = 5$) and 6-month-old ($n = 5$) WAG/Rij slices superfused with control medium. In addition, more-pronounced effects were identified by testing the effects induced by 100 μM LEV in these two age groups ($n = 3$ and 5 slices from 3- and 6-month-old animals, respectively). Figure 4C and D summarizes the percentage reduction in IOS intensity and area size seen during application of these two doses of LEV. It is worth noting that the decreases in IOS intensity and area size induced by either 50 or 100 μM LEV (which are considered clinically relevant concentrations; cf., 37) were more pronounced ($p < 0.02$) in 6- month-old than in 3-month-old WAG/Rij slices.

We also analyzed the changes induced by LEV on the IOS patterns induced by single-shock stimuli in 3- and 6-month-old WAG/Rij slices that were superfused with 4-AP–containing medium. In these experiments, we tested the effects of 50, 100, 200, and 500 μM LEV in six, three, four, and five slices from 3-month-old WAG/Rij rats as well as in eight, five, three, and four slices from 6-month-old WAG/Rij animals. As shown in the dose–response histograms in Fig. 4E and F, increasing LEV concentrations caused stronger reductions in both IOS peak intensity and area size. In addition, LEV concentrations induced decreases in IOS peak intensity and area size that were more pronounced in 6-month-old than in 3-month-old WAG/Rij slices. However, these decreases were significantly different between the two age groups only for the area reductions.

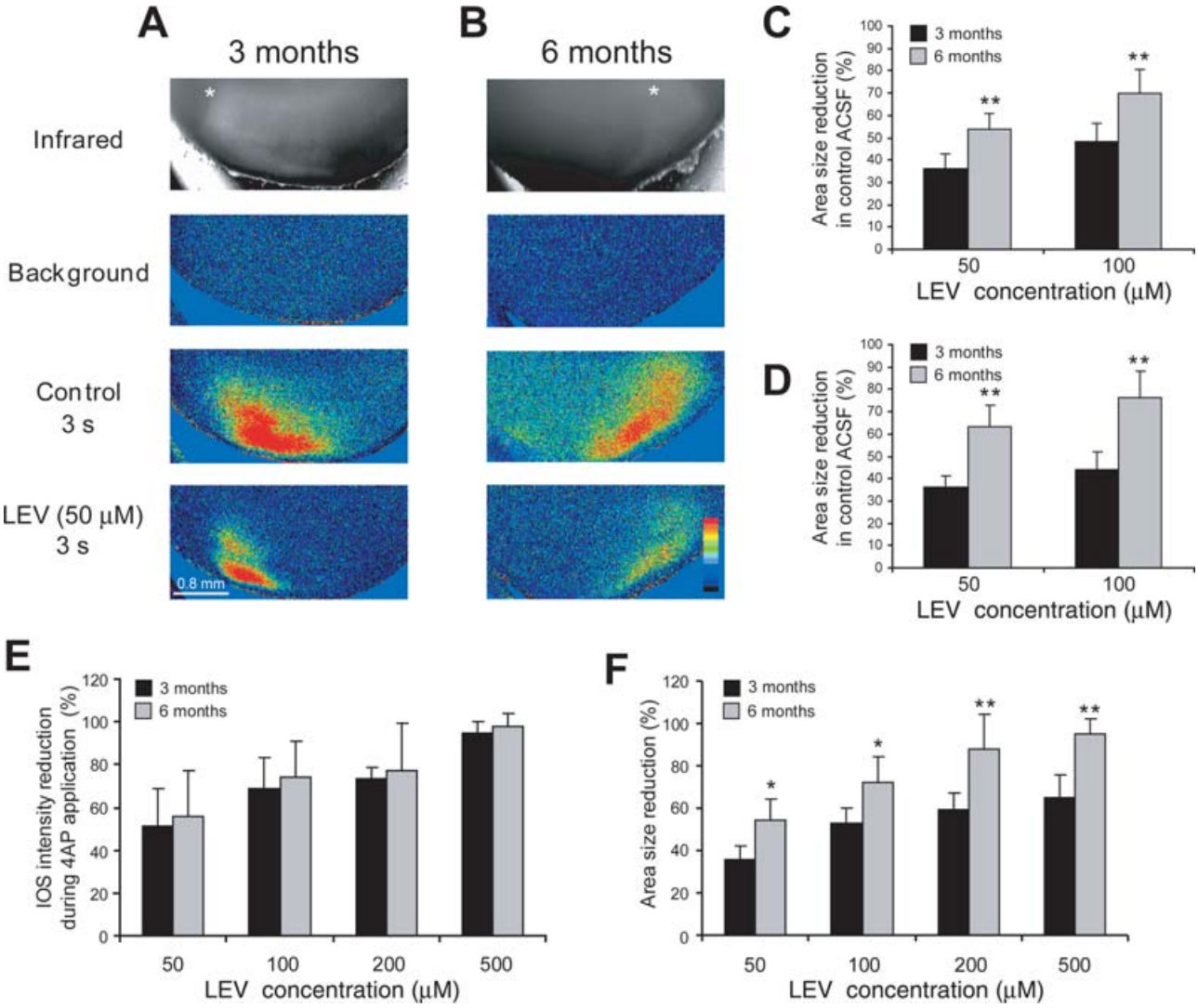

FIG. 4. A, B: Effects induced by 50 μM levetiracetam (LEV) on the intrinsic optical signals (IOSs) changes induced in 3- and 6-month-old neocortical WAG/Rij slices by single-shock stimuli in control artificial cerebrospinal fluid. Note that LEV causes a decrease in IOS intensity and area size in both experiments. **C, D:** Quantification of the reduction in intensity and area size caused by 50 and 100 μM LEV. **E, F:** Dose-responses of the effects induced by LEV in WAG/Rij slices from the two age groups. In the presence of 4-AP–containing medium. Note that the percentage reductions are always more pronounced in 6-month-old WAG/Rij slices, but these differences are significant only for the area reductions induced by LEV doses of 200 and 500 μM.

DISCUSSION

The present findings further identify an increase in neocortical network excitability that characterizes WAG/Rij rats, and in particular, somatosensory neocortical networks in slices that were obtained from 6-month-old animals. It has been documented in this genetic model that absence seizures (and the accompanying generalized SW discharges) occur spontaneously in all animals >180 days old. Moreover, several studies of SW discharges in either GAERS or WAG/Rij rats have identified a primary role of this cortical area in the initiation of generalized SW discharges (15,18,20). Our conclusions rest on (a) the ability of single-shock stimuli to elicit widespread IOS changes in WAG/Rij rat slices superfused with control medium, whereas stimulus trains were required to induce IOS increases in NEC tissue under similar conditions (cf., Fig. 1); (b) the fact that age-dependent decreases in IOS patterns were identified in NEC slices (both in control and in 4-AP–containing medium), whereas no change (in control) or an increase (in the presence of 4-AP) characterized the IOS changes recorded from WAG/Rij rat slices (cf., Figs. 1 and 2); and (c) the evidence that both IOS intensities and areas, regardless of age group or experimental condition, were larger in WAG/Rij rat slices. In addition, we found that the spread of the IOS recorded from 6-month-old WAG/Rij slices depended on the anatomical integrity of superficial neocortical layers (cf. Fig. 3). Finally, we discovered that clinically relevant concentrations of the

novel AED LEV can exert clear depressant effects on the IOS changes recorded from WAG/Rij slices superfused with either control or 4-AP–containing medium (cf. Fig. 4).

Age-dependent changes in IOSs recorded from NEC and WAG/Rij rat neocortical slices

We observed in 3 month-old NEC slices superfused with control aCSF, after brief stimulus trains, the same IOS pattern previously reported in 30- to 40-day-old rat tissue (26,36); this pattern corresponds to a columnar representation with a peak increase localized in the superficial layers. In contrast, the IOSs induced by similar stimulus trains in 6-month-old NEC slices lacked a clear delimitation and had peak increases and area sizes that were significantly lower and smaller, respectively. Moreover, similar decreases were identified when NEC slices were analyzed in the presence of 4-AP. We are inclined to interpret these changes as reflecting a physiologic reduction of the activity linked to aging. It is indeed well established that aging is characterized by a decrease of excitatory (38,39) and inhibitory (40–42) synaptic substrates, dendritic spine regression (43), and diminished number of synaptophysin immunoreactive presynaptic boutons (44,45).

In contrast to that identified in NEC tissue, WAG/Rij slices were characterized by an age-dependent increase in both IOS intensity and area. Interestingly, these changes involved mainly the superficial layers of the epileptic WAG/Rij slices, a location where Luhmann et al. (46) found a decrease in γ-aminobutyric acid $(GABA)_A$ receptor–mediated inhibition. Moreover, Dodt et al. (26) reported that the columnar IOS pattern identified in young animals (and confirmed by us in 3-month-old NEC slices; cf., Fig. 1A) is disrupted by bath application of the $GABA_A$-receptor antagonist bicuculline. Indeed, these IOS developmental characteristic are in keeping with evidence indicating that WAG/Rij rats consistently generate absence seizures after 6 months (22).

Spread of the IOS responses in 6-month-old WAG/Rij neocortex

Supragranular layers appear to play an important role in the propagation through the neocortex of the activity identified with IOS recordings in 6-month-old WAG/Rij rats. Similar conclusions were obtained by Albowitz and Kuhnt (47), who analyzed with voltage-sensitive dyes the spread of epileptiform activity in guinea-pig neocortical slices. In addition, Alefeld et al. (48) found that horizontal fibers running through layer I are involved in the transfer of synchronized epileptiform activity to distant neocortical regions; these authors proposed that layer I inputs on the distal apical dendrites of layer V bursting neurons may support epileptiform synchronization. These cells are indeed known to play a major role in the generation and propagation of neocortical epileptiform activity (49,50). It should, however, be emphasized that these findings were obtained by analyzing in vitro focal epileptogenesis induced in normal neocortical tissue by bath application of $GABA_A$-receptor antagonists. Hence, to the best of our knowledge, the evidence obtained in WAG/Rij neocortical slices treated with low concentrations of 4-AP identifies for the first time the role of supragranular layers in ensuring the spread of synchronous activity in a genetic model of generalized epilepsy. The role of neocortical connections in the initiation and propagation of SW discharge in the WAG/Rij model has been clearly identified in vivo by Meeren et al. (18).

LEV reduces IOSs in WAG/Rij rat neocortical slices

The patterns of IOS changes recorded in neocortical slices obtained from 3- and 6-month-old WAG/Rij were influenced by bath application of the novel AED LEV, both in control medium and in the presence of 4-AP. These effects, which corresponded to reductions in both IOS intensity and area size, were seen with LEV concentrations that are considered to be clinically relevant (i.e, 50 μM; cf. 37). In addition, the LEV-induced decreases identified in slices superfused with control medium were significantly more pronounced in 6-month-old tissue, which corresponds to the age when all WAG/Rij rats generate spontaneous SW discharges in vivo (22). Interestingly, this age-dependent characteristic was seen in the presence of 4-AP, only for the effects exerted by LEV on IOS area size. Although we do not have any explanation for this difference, it should be emphasized that 4-AP is known to increase transmitter release at both excitatory and inhibitory terminals (51,52), whereas LEV is able to bind to a synaptic vesicle protein (53).

LEV has been tested on epileptiform discharges recorded in vitro from hippocampal slices treated with convulsants or epileptogenic media (see for review, 54). These studies have shown that doses of LEV similar to those used here in WAG/Rij neocortical slices can reduce epileptiform synchronization in the CA3 area of hippocampal slices superfused with high-K^+/low-Ca^{2+} aCSF (37), 4-AP (55), or the $GABA_A$-receptor antagonist bicuculline (56). It was also shown in this last study that LEV inhibits the development of bicuculline-induced epileptiform bursting without altering normal synaptic transmission (56). Finally, Gorji et al. (57) identified similar antiepileptogenic effects of LEV in human neocortical slices treated with bicuculline.

Previous reports indicated that LEV induces anticonvulsant effects in audiogenic-seizure-prone, as well as in the GAERS rats (58). Moreover, similar evidence has been recently obtained by testing the effects of LEV on generalized SW discharges in WAG/Rij rats in vivo (59). It is worth noting that in the GAERS study, LEV abolished SW discharges without producing detectable behavioral effects or influencing the background EEG activity (58), which is in agreement with preliminary data indicating

that low concentrations (50–100 μM) of LEV do not influence the IOS changes generated by either 3- or 6-month-old NEC slices in normal aCSF (G. D'Arcangelo and M. Avoli, unpublished results). Overall, both these in vivo studies and our present in vitro evidence support the clinical use of LEV in primary generalized epileptic disorders (60,61).

REFERENCES

1. Panayiotopoulos CP. Typical absence seizures and their treatment. *Arch Dis Child* 1999;81:351–5.
2. Avoli M, Rogawsk MA, Avanzini G. Generalized epileptic disorders: an update. *Epilepsia* 2001;42:445–57.
3. Crunelli V, Leresche N. Childhood absence epilepsy: genes, channels, neurons and networks. *Nat Rev Neurosci* 2002;3:371–82.
4. Vergnes M, Marescaux C, Depaulis A, et al. Spontaneous spike-wave discharges in Wistar rats: a model of genetic generalized convulsive epilepsy. In: Avoli M, Gloor P, Kostopoulos G, et al., eds. *Generalized epilepsy*: *neurobiological approaches*. Boston: Birkhäuser, 1990:238–53.
5. van Luijtelaar ELJM, Coenen AML. Two types of electrocortical paroxysms in an inbred strain of rats. *Neurosci Lett* 1986;70:393–7.
6. Coenen AML, van Luijtelaar ELJM. Genetic animal models for absence epilepsy: a review of the WAG/Rij strain of rats. *Behav Genet* 2003;33:635–55.
7. Lennox WG, Lennox MA. *Epilepsy and related disorders*. Boston: Little Brown, 1960.
8. Metrakos K, Metrakos JD. Genetics of convulsive disorders, II: genetic and electroencephalographic studies in centrencephalic epilepsy. *Neurology* 1961;11:464–83.
9. Avoli M, Gloor P, Kostopoulos G, et al. An analysis of penicillin-induced generalized spike and wave discharges using simultaneous recordings of cortical and thalamic single neurons. *J Neurophysiol* 1983;50:819–37.
10. Neckelmann D, Amzica F, Steriade M. Spike-wave complexes and fast components of cortically generated seizures, III: synchronizing mechanisms. *J Neurophysiol* 1998;80:1480–94.
11. Steriade M, Amzica F, Neckelmann D, et al. Spike-wave complexes and fast components of cortically generated seizures, II: extra- and intracellular patterns. *J Neurophysiol* 1998;80:1456–79.
12. Timofeev I, Grenier F, Steriade M. Spike-wave complexes and fast components of cortically generated seizures, IV: paroxysmal fast runs in cortical and thalamic neurons. *J Neurophysiol* 1998;80:1495–513.
13. Steriade M, Contreras D. Spike-wave complexes and fast components of cortically generated seizures, I: role of neocortex and thalamus. *J Neurophysiol* 1998;80:1439–55.
14. Charpier S, Leresche N, Deniau JM, et al. On the putative contribution of GABA(B) receptors to the electrical events occurring during spontaneous spike and wave discharges. *Neuropharmacology* 1999;38:1699–706.
15. Pinault D. Cellular interactions in the rat somatosensory thalamocortical system during normal and epileptic 5-9 Hz oscillations. *J Physiol (Lond)* 2003;552:881–905.
16. Seidenbecher T, Staak R, Pape HC. Relations between cortical and thalamic cellular activities during absence seizures in rats. *Eur J Neurosci* 1998;10:1103–12.
17. Vergnes M, Boehrer A, Nehlig A. Developmental characteristics of picrotoxin-induced convulsions in rats with genetic absence epilepsy. *Exp Neurol* 2003;184:549–51.
18. Meeren HK, Pijn JP, van Luijtelaar EL, et al. Cortical focus drives widespread corticothalamic networks during spontaneous absence seizures in rats. *J Neurosci* 2002;22L:1480–95.
19. Nersesyan H, Hyder F, Rothman DL, et al. Dynamic fMRI and EEG recordings during spike-wave seizures and generalized tonic-clonic seizures in WAG/Rij rats. *J Cereb Blood Flow Metab* 2004;24:589–99.
20. Manning JP, Richards DA, Leresche N, et al. Cortical-area specific block of genetically determined absence seizures by ethosuximide. *Neuroscience* 2003;123:5–9.
21. D'Arcangelo G, D'Antuono M, Biagini G, et al. Thalamocortical oscillations in a genetic model of absence seizures. *Eur J Neurosci* 2002;16:2383–93.
22. Coenen AML, van Luijtelaar ELJM. The WAG/Rij rat model for absence epilepsy: age and sex factors. *Epilepsy Res* 1987;1:97–301.
23. MacVicar B, Hochman D. Imaging of synaptically evoked intrinsic optical signals in hippocampal slices. *J Neurosci* 1991;11:1458–69.
24. Andrew RD, MacVicar B. Imaging cell volume changes and neuronal excitation in the hippocampal slice. *Neuroscience* 1994;62:371–83.
25. Hochman D, Baraban S, Owens J, et al. Dissociation of synchronization and excitability in furosemide blockade of epileptiform activity. *Science* 1995;270:99–102.
26. Dodt HU, D'Arcangelo G, Pestel E, et al. The spread of excitation in neocortical columns visualized with infrared-darkfield videomicroscopy. *Neuroreport* 1996;7:1553–8.
27. Buchheim K, Schuchmann S, Siegmund H, et al. Intrinsic optical signal measurements reveal characteristic features during different forms of spontaneous neuronal hyperactivity associated with ECS shrinkage in vitro. *Eur J Neurosci* 1999;11:1877–82.
28. Klitgaard H. Levetiracetam: the preclinical profile of a new class of antiepileptic drugs? *Epilepsia* 2001;42(suppl 4):13–8.
29. Marson AG, Hutton JL, Leach JP, et al. Levetiracetam, oxcarbazepine, remacemide and zonisamide for drug resistant localization-related epilepsy: a systematic review. *Epilepsy Res* 2001;46:259–70.
30. Leppik IE. Levetiracetam: clinical use. In: Levy RH, Mattson RH, Meldrum BS, et al., eds. *Antiepileptic drugs.* 5th ed. Philadelphia: Lippincott Williams & Wilkins, 2002:433–41.
31. Sullivan JE, Dlugos DJ. Idiopathic generalized epilepsy. *Curr Treat Options Neurol* 2004;6:231–42.
32. Drinkenburg WH, van Luijtelaar EL, van Schaijk WJ, et al. Aberrant transients in the EEG of epileptic rats: a spectral analytical approach. *Physiol Behav* 1993;54:779–83.
33. Midzianovskaia IS, Kuznetsova GD, Coenen AM, et al. Electrophysiological and pharmacological characteristics of two types of spike-wave discharges in WAG/Rij rats. *Brain Res* 2001;911:62–70.
34. Paxinos G, Watson C. *The rat brain in stereotaxic coordinates*. 4th ed. San Diego: Academic Press, 1998.
35. D'Arcangelo G, Tancredi V, Avoli M. Intrinsic optical signals and electrographic seizures in the rat limbic system. *Neurobiol Dis* 2001;8:993–1005.
36. D'Arcangelo G, Tancredi V, Onofri F, et al. Interleukin-6 inhibits neurotransmitter release and the spread of excitation in the rat cerebral cortex. *Eur J Neurosci* 2000;12:1241–52.
37. Margineanu DG, Klitgaard H. Inhibition of neuronal hypersynchrony in vitro differentiates levetiracetam from classical antiepileptic drugs. *Pharmacol Res* 2000;42:281–5.
38. Potier B, Poindessous-Jazat F, Dutar P, Billard JM. NMDA receptor activation in the aged rat hippocampus. *Exp Gerontol* 2000;35:1185–99.
39. Segovia G, Porras A, Del Arco A, et al. Glutamatergic neurotransmission in aging: a critical perspective. *Mech Ageing Dev* 2001;122:1–29.
40. Mhatre MC, Ticku MK. Aging related alterations in $GABA_A$ receptor subunit mRNA levels in Fisher rats. *Mol Brain Res* 1992;14:71–8.
41. Post-Munson DJ, Lum-Ragan JT, Mahle CD, et al. Reduced bicuculline response and GABAA agonist binding in aged rat hippocampus. *Neurobiol Aging* 1994;15:629–33.
42. Poe BH, Linville C, Brunso-Bechtold J. Age-related decline of presumptive inhibitory synapses in the sensorimotor cortex as revealed by the physical disector. *J Comp Neurol* 2001;439:65–72.
43. Duan H, Wearne SL, Rocher AB, et al. Age-related dendritic and spine changes in corticocortical projecting neurons in macaque monkeys. *Cereb Cortex* 2003;19:950–61.
44. Chen KS, Masliah E, Mallory M, et al. Synaptic loss in cognitively impaired aged rats is ameliorated by chronic human nerve growth factor infusion. *Neuroscience* 1995;68:19–27.
45. Wong TP, Campbell PM, Ribeiro-da-Silva A, et al. Synaptic

numbers across cortical laminae and cognitive performance of the rat during ageing. *Neuroscience* 1998;84:403–12.
46. Luhmann HJ, Mittmann T, van Luijtelaar G, et al. Impairment of intracortical GABAergic inhibition in a rat model of absence epilepsy. *Epilepsy Res* 1995;22:43–51.
47. Albowitz B, Kuhnt U. Epileptiform activity in the guinea-pig neocortical slice spreads preferentially along supragranular layers: recordings with voltage-sensitive dyes. *Eur J Neurosci* 1995;7:1273–84.
48. Alefeld M, Sutor B, Luhmann HJ. Pattern and pharmacology of propagating epileptiform activity in mouse cerebral cortex. *Exp Neurol* 1998;153:113–22.
49. Connors BW. Initiation of synchronized neuronal bursting in neocortex. *Nature* 1984;310:685–7.
50. Chagnac-Amitai Y, Connors BW. Synchronized excitation and inhibition driven by intrinsically bursting neurons in neocortex. *J Neurophysiol* 1989;62:1149–62.
51. Buckle PJ, Haas HL. Enhancement of synaptic transmission by 4-aminopyridine in hippocampal slices of the rat. *J Physiol* 1982;326:109–22.
52. Perreault P, Avoli M. Effects of low concentrations of 4-aminopyridine on CA1 pyramidal cells of the hippocampus. *J Neurophysiol* 1989;61:953–70.
53. Lynch BA, Lambeng N, Nocka K, et al. The synaptic vesicle protein SV2A is the binding site for the antiepileptic drug levetiracetam. *Proc Natl Acad Sci USA* 2004;101:9861–6.
54. Margineanu D-G, Klitgaard H. Levetiracetam: mechanisms of action. In: Levy RH, Mattson RH, Meldrum BS, et al., eds. *Antiepileptic drugs.* 5th ed. Baltimore: Lippincott Williams & Wilkins, 2002:19–427.
55. Leniger T, Thone J, Bonnet U, et al. Levetiracetam inhibits Na^{+}-dependent $Cl^{-}/HCO3^{-}$ exchange of adult hippocampal CA3 neurons from guinea-pigs. *Br J Pharmacol* 2004;142:1073–80.
56. Birnstiel S, Wülfert E, Beck SG. Levetiracetam (ucbL059) affects in vitro models of epilepsy in CA3 pyramidal neurons without altering normal synaptic transmission. *Naunyn Schmiedebergs Arch Pharmacol* 1997;356:611–8.
57. Gorji A, Hohling JM, Madeja M, et al. Effect of levetiracetam on epileptiform discharges in human neocortical slices. *Epilepsia* 2000;43:1480–7.
58. Gower AJ, Hirsch E, Boehrer A, et al. Effects of levetiracetam, a novel antiepileptic drug, on convulsant activity in two genetic rat models of epilepsy. *Epilepsy Res* 1995;22:207–13.
59. Bouwman BM, van Rijn CM. Effects of levetiracetam on spike and wave discharges in WAG/Rij rats. *Seizure* 2003;13:591–4.
60. Cohen J. Levetiracetam monotherapy for primary generalised epilepsy. *Seizure* 2003;12:150–3.
61. Weber S, Beran RG. A pilot study of compassionate use of levetiracetam in patients with generalised epilepsy. *J Clin Neurosci* 2004;11:728–31.